RESEARCH ARTICLE

Influence of seasonal sea-ice loss on Arctic precipitation δ18O: a GCM-based analysis of monthly data

Wenxuan Song, Zhongfang Liu, Haimao Lan & Xiaohe Huan
State Key Laboratory of Marine Geology, Tongji University, Shanghai, China

Abstract

Rapid Arctic warming and sea-ice loss have intensified the Arctic hydrological cycle, increasing local evaporation and precipitation. Stable water isotopes as environmental tracers can provide useful insights into the Arctic hydrological cycle. However, the paucity of isotopic observations in the Arctic has limited our understanding of the hydrological changes. Here, we use an isotope-enabled atmospheric general circulation model (IsoGSM) combined with the Global Network of Isotopes in Precipitation (GNIP) observations to investigate the relationship between sea-ice changes and Arctic precipitation $\delta^{18}O$ ($\delta^{18}O_p$) to reveal the relative influence of local air temperature and evaporation on Arctic summer and winter $\delta^{18}O_p$. We find that the Arctic $\delta^{18}O_p$ is negatively correlated with sea-ice concentration but positively with air temperature. Sea-ice loss leads to enriched Arctic $\delta^{18}O_p$ through enhanced local evaporation and warming, but the relative importance of these processes varies between seasons. During summer, both local evaporation and warming contribute equally to $\delta^{18}O_p$ changes. In contrast, winter $\delta^{18}O$ is predominantly driven by air temperature. This work improves our understanding of how Arctic precipitation isotopes respond to sea-ice changes and has implications for the Arctic hydrological cycle and palaeotemperature reconstructions.

Keywords
Precipitation isotope; Arctic warming; sea ice; local evaporation; hydrological cycle; palaeotemperature reconstruction

Correspondence
Zhongfang Liu, Tongji University, 1239 Siping Road, Yangpu District, 200092 Shanghai, China. E-mail liuzf406@gmail.com

Abbreviations
ASO: August–September–October
BKS: Barents–Kara seas
CMIP5: Coupled Model Intercomparison Project Phase 5
DJF: December–January–February
GCM: general circulation model
GNIP: Global Network of Isotopes in Precipitation
HYSPLIT: Hybrid Single-Particle Lagrangian Integrated Trajectory (model)
IsoGSM: Isotope-incorporated Global Spectral Model
JJA: June–July–August
NCEP: National Centers for Environmental Prediction (USA)
NSIDC: National Snow and Ice Data Center (USA)
SIC: sea-ice concentration

To access the supplementary material, please visit the article landing page

Introduction

Over the past four decades, the Arctic has been warming at least twice as fast as the global average, a phenomenon referred to as 'Arctic amplification' (Blunden & Arndt 2012; Cohen et al. 2014). Arctic sea ice is melting at an unprecedented rate, with summer sea-ice predicted to disappear by the middle of this century (Stroeve et al. 2012; Overland & Wang 2013) or even as early as 2035 (Voosen 2020). Rapid Arctic warming and sea-ice loss have led to an intensification of the Arctic hydrological cycle (Vihma et al. 2016; Ford & Frauenfeld 2022), which is characterized by increased melting and local evaporation (Screen & Simmonds 2010; Kopec et al. 2016), enhanced poleward moisture transport (Graversen et al. 2008; Screen & Simmonds 2012), as well as increased precipitation (Bintanja & Selten 2014; Kopec et al. 2016). Because of the limited availability of in situ and remote-sensing observations, our current understanding of the Arctic hydrological cycle is largely based on atmospheric reanalysis and model simulations (Boisvert et al. 2018). Therefore, constraining the Arctic hydrological cycle in response to sea-ice changes remains challenging.

Precipitation isotopes ($\delta^{18}O$ and δD) and its secondary parameter deuterium excess (d-excess, defined as d-excess = $\delta D - 8\times\delta^{18}O$; Dansgaard 1964) provide an alternative approach that can help elucidate the hydrological cycle across a range of spatial and temporal scales (Dansgaard 1964; Gat et al. 1994; Galewsky et al. 2016; Bowen et al. 2019). At high latitudes, precipitation isotope variation is traditionally regarded as a reflection of temperature-dependent fractionation (Dansgaard 1964), with significant positive correlation between $\delta^{18}O$ and air temperature: the so-called 'temperature effect'. This

Citation: *Polar Research* 2023, *42*, 9751, http://dx.doi.org/10.33265/polar.v42.9751

temperature/$\delta^{18}O$ relationship underlies an important method for the reconstruction of palaeotemperature (Jouzel et al. 1997). However, observations have indicated that precipitation $\delta^{18}O$ does not consistently covary with local air temperature (Bowen 2008; Bonne et al. 2014; Cluett et al. 2021), suggesting other processes such as moisture source changes can affect precipitation $\delta^{18}O$ variation (Kurita 2011; Klein et al. 2015). The d-excess parameter, which is controlled mainly by the kinetic fractionation associated with evaporation at the moisture source region (Merlivat & Jouzel 1979), can provide information about moisture sources.

The impacts of Arctic sea-ice loss on the local hydrological cycle are supposed to be reflected in the variations of water vapour and precipitation $\delta^{18}O$ and d-excess (Kurita 2011; Klein et al. 2015; Klein & Welker 2016; Kopec et al. 2016; Faber et al. 2017; Sime et al. 2019; Mellat et al. 2021). An earlier study indicated that the evaporated moisture from the Arctic Ocean tends to have higher d-excess values than those advected from lower latitudes (Kurita 2011). However, this contrasts with many recent studies that showed lower d-excess values in both Arctic water vapour (Klein et al. 2015; Klein & Welker 2016) and precipitation (Kopec et al. 2016) in response to local evaporation due to sea-ice loss. These disagreements may reflect the great complexity of Arctic sea-ice changes across regions and seasons (Liu et al. 2021; Liu et al. 2022) or poor isotope observations that are relatively short-term and sparse in the Arctic, which has posed substantial challenges to diagnosing the Arctic hydrological cycle using stable water isotopes.

Despite these disagreements, most previous studies focus on changes in d-excess responses to Arctic sea-ice loss (Kurita 2011; Klein et al. 2015; Klein & Welker 2016; Kopec et al. 2016), but a direct link between sea-ice loss and Arctic precipitation isotopes (e.g., $\delta^{18}O$) has yet to be substantiated. This is in part due to the limited observations of precipitation isotopes in the Arctic, particular in the regions of sea-ice coverage. Although the pan-Arctic precipitation isotope network recently developed by Mellat et al. (2021) provides important insight into the impacts of sea-ice variation and associated moisture dynamics on Arctic precipitation isotopes from event-based sampling, it comprises exclusively land stations and has a profile of only short-term isotope records.

To circumvent this limitation, state-of-the-art GCMs equipped with water isotope tracers have been used to investigate the mechanistic links between sea ice and Arctic precipitation isotopes (Faber et al. 2017; Sime et al. 2019). Most modelling efforts focus on annual timescales (Sime et al. 2013; Faber et al. 2017; Sime et al. 2019), which may mask some important seasonal isotopic signals (Bowen 2008), given strong seasonality in Arctic sea-ice changes. Moreover, GCM simulations have suggested more enriched Arctic precipitation $\delta^{18}O$ in response to sea-ice loss due to enhanced local evaporation (Sime et al. 2013; Faber et al. 2017; Sime et al. 2019), as opposed to a recent observational study that showed more depleted $\delta^{18}O_p$ due to sea-ice decline (Mellat et al. 2021).

In this study, we combine IsoGSM simulations (Yoshimura & Kanamitsu 2008) and monthly observations of SIC from the NSIDC to investigate the effects of seasonal sea-ice loss on Arctic $\delta^{18}O_p$ over the period 1979–2020. We focus exclusively on $\delta^{18}O_p$; d-excess is not included in our analysis because GCM can hardly reproduce precipitation d-excess. Our aims are: (1) to reveal the response of Arctic $\delta^{18}O_p$ to seasonal sea-ice changes; (2) to assess the relative influence of local evaporation and warming due to sea-ice loss on Arctic $\delta^{18}O_p$; and (3) to elucidate how the $\delta^{18}O_p$/SIC relationship might be used for the Arctic hydrological cycle and palaeotemperature reconstructions. To this end, we first quantify the performance of IsoGSM in the Arctic using observed temperature and $d^{18}O_p$ from GNIP (IAEA/WMO 2019). We then explore the relationships of Arctic $\delta^{18}O_p$ with SIC and local air temperature and discuss the relative importance of air temperature and local evaporation in determining Arctic $\delta^{18}O_p$ for different seasons. Finally, we discuss the potential implications of this work for the Arctic hydrological cycle and $\delta^{18}O$-based palaeotemperature reconstructions.

Data and methods

Observations

Monthly SIC data used in this study are derived from the NSIDC (available at https://nsidc.org/data/G02202/versions/4; Meier et al. 2021). Of the several different SIC products provided by the NSIDC, we chose the latest (version 4) of the SIC data for our analysis. This data set provides a climate data record of SIC from passive microwave satellite observations from November 1978 to December 2020, with a horizontal resolution of 25 km × 25 km.

To evaluate the performance of the IsoGSM, monthly $\delta^{18}O_p$ and air temperature from 20 Arctic GNIP stations located north of 65°N are used in this study (Supplementary Fig. S1 and Supplementary Table S1). These stations span a broad geographic area but have record lengths varying from five to 42 years within the 1979–2020 period. The GNIP database provides isotopic composition of precipitation ($\delta^{18}O$ and δD) and meteorological data collected on a monthly basis from a global network of stations. Most GNIP isotope data before 2010 were measured by isotope-ratio mass spectrometry and later on by laser spectroscopy. All isotope values are expressed as parts per thousand of their deviation relative to the Vienna Standard Mean Ocean Water and Standard Light Antarctic Precipitation.

IsoGSM model

Precipitation isotope simulations were performed using the IsoGSM, a current-generation GCM that incorporates water isotopes into the Scripps Experimental Climate Prediction Center's global spectral atmospheric general circulation model (Yoshimura et al. 2008). The model has 28 vertical levels and a spectral horizontal of about 200 km. The model is forced with prescribed sea-surface temperatures and sea-ice conditions from the optimal interpolation daily data set (Yoshimura & Kanamitsu 2008) provided by the NCEP (Reynolds et al. 2007). To accurately reproduce the observed climate conditions, the simulations were spectrally nudged at six-hour intervals to wind and temperature fields from the NCEP reanalysis (Kanamitsu et al. 2002). Such nudging enables the IsoGSM to well reproduce monthly precipitation and its isotopic composition (Yoshimura et al. 2008; Wei et al. 2016). Here, we report a 42-year record (1979–2020) $\delta^{18}O_p$ and air temperature from IsoGSM simulations.

Air mass back-trajectory analysis

Air mass back-trajectory analysis was used to determine the influence of moisture sources due to sea-ice changes on Arctic $\delta^{18}O_p$. Back trajectories were calculated for the months of maximum and minimum sea-ice coverage during summer and winter seasons using the HYSPLIT model, version 4.0 (Draxler & Hess 1998; Adler et al. 2003; Stein et al. 2015) with the NCEP reanalysis data. We focused on the trajectories arriving at 500 m above mean sea level, which corresponds to the height of air mass movement in the Arctic (Puntsag et al. 2016; Leroy-Dos Santos et al. 2020) and has been used to assess the influence of moisture sources on Arctic $\delta^{18}O_p$ (Puntsag et al. 2016; Bailey et al. 2021). Each trajectory was traced back for seven days for winter and 15 days for summer, which represent the mean residence time of water vapour over the whole Arctic (van der Ent & Tuinenburg 2017). All trajectories were clustered using an angle-based distance matrix to identify the major moisture sources in the Beaufort Sea and the BKS, where sea-ice decline is strongest in summer and winter seasons, respectively (Liu et al. 2021; Liu et al. 2022). To facilitate our analysis, two sites in the region, namely, the Beaufort Sea (72°N, 155°W) and the BKS (78°N, 60°E), were selected for trajectory calculations.

Results

Model evaluation

To assess the performance of the IsoGSM, we first compared the long-term annual mean temperature and $\delta^{18}O_p$ from the simulations with observed station data from the GNIP across the Arctic north of 65° N (Fig. 1). The IsoGSM successfully reproduces the observed spatial variability of temperatures, with a correlation of 0.94 (Fig. 1a). However, the observed station temperatures are somewhat overestimated. The modelled annual mean temperature is −9.54 °C, generally higher than the observed value of −10.54 °C. This small offset between simulations and observations derives largely from a systematic overestimate in colder regions such as the central Arctic and northern Greenland, where warm biases can be up to 2 °C. The overestimation of temperature in the Arctic is not unique to the IsoGSM model but occurs in most CMIP5 models (Huang et al. 2019) and is mainly due to complex radiative feedbacks, which are not well resolved by the models.

The model mimics well the large-scale spatial pattern in the observed station $\delta^{18}O_p$. A spatial correlation analysis indicates that the model accounts for 81% of the observed spatial variance in $\delta^{18}O_p$, with a mean positive bias of 4.40 ‰ (Fig. 1b). This positive bias largely reflects some substantial overestimates of $\delta^{18}O_p$ in colder (or higher latitude) regions where positive biases of 5–10‰ are observed. These overestimates are not unexpected, given that the model simulates higher temperature in these stations. In addition, the positive $\delta^{18}O_p$ biases are also found in other models and are due partly to the influence of amplified local feedback in the model (Nan et al. 2021), but the detailed processes still need further investigation.

We also evaluated the capability of the model to represent the temporal behaviours of observed temperature and $\delta^{18}O_p$ by comparing them with observations at Danmarkshavn (Greenland) and Ny-Ålesund (Svalbard), which have the longest and continuous temperature and $\delta^{18}O_p$ records. As shown in Fig. 1c and d, the simulated monthly temperatures strongly resemble the observed counterparts at both stations (r > 0.96). The simulated $\delta^{18}O_p$ values are moderately (r = 0.78 at Danmarkshavn and 0.47 at Ny-Ålesund) correlated with observations, although the correlations are significant at the 95% confidence. The low $\delta^{18}O_p$ correlation at Ny-Ålesund is complicated, potentially arising from the poor representation of atmospheric circulation by the IsoGSM that is forced by only the observed sea-surface conditions (Yoshimura et al. 2008) or from uncertainties in GNIP isotope data due to sampling and isotopic

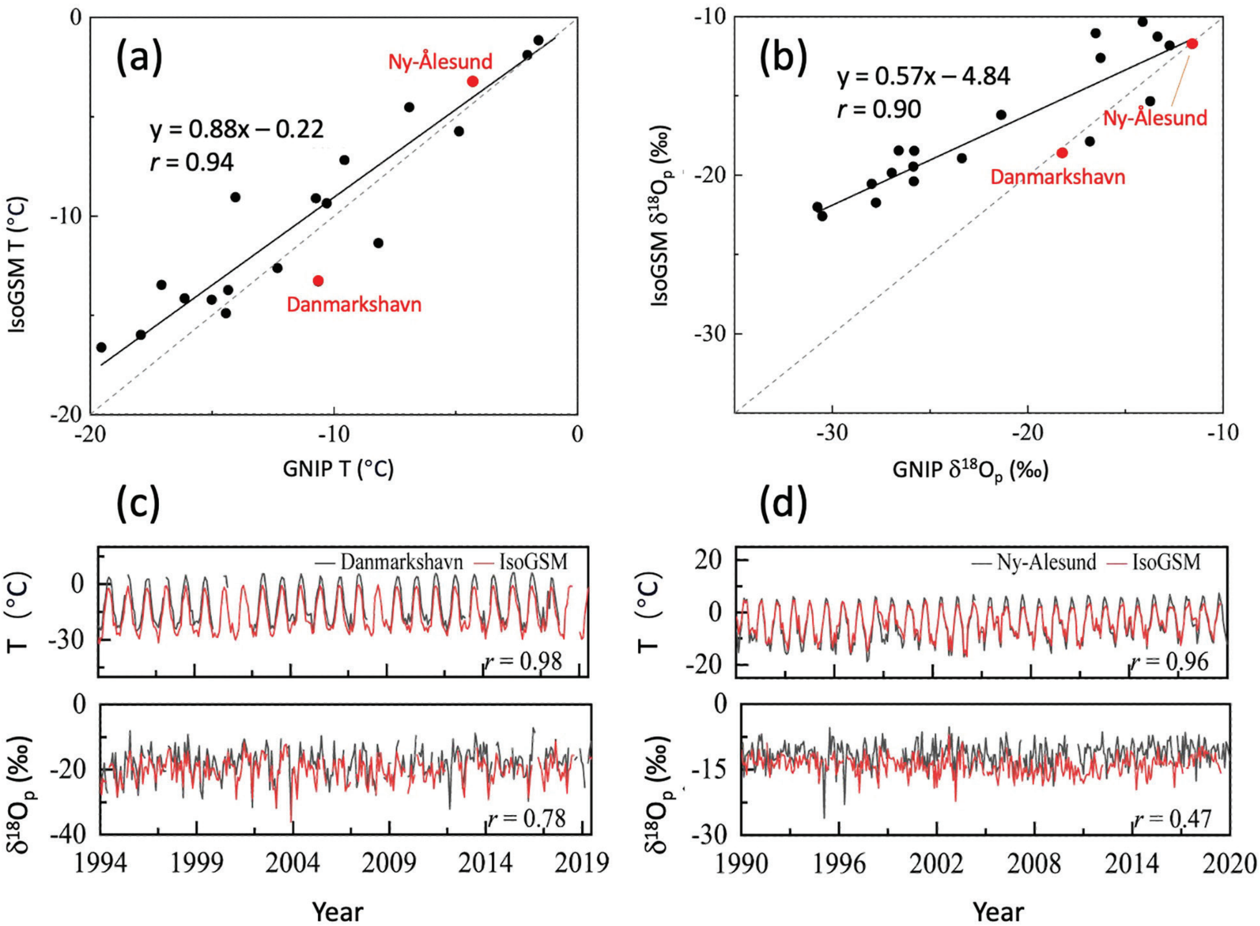

Fig. 1 Comparisons of (a) annual temperature and (b) $\delta^{18}O_p$ between simulations and observations at co-located GNIP station across the Arctic (65–90° N). Monthly time series of simulated and observed temperatures and $\delta^{18}O_p$ at (c) Danmarkshavn site (76.8°N, 18.7°W) and (d) Ny-Ålesund site (78.9°N, 11.9°E).

measurements (Fröhlich et al. 2002). Given good performance of the model in reproducing $\delta^{18}O_p$ at Danmarkshavn and other non-Arctic stations (Liu et al. 2014), the bias in $\delta^{18}O_p$ at Ny-Ålesund largely reflects uncertainties in observed isotopic data, which is also supported by a poor correlation between the observed temperature and $\delta^{18}O_p$ at Ny-Ålesund (Supplementary Fig. S2). We also note that both temperatures and $\delta^{18}O_p$ are slightly underestimated at the two stations, especially in summer. This contrasts with the positive biases in the seasonal averages shown in Fig. 1a and b, likely largely reflecting different model representations across regions and seasons.

As shown earlier, the IsoGSM produces an overall realistic representation of the spatial and temporal variations in Arctic air temperature and $\delta^{18}O_p$, but with modest biases in colder (or higher latitude) regions. These regional biases are also found in other models and arise largely from complex radiative feedback processes and stable boundary layer dynamics in the Arctic (Vihma et al. 2014), which are not well resolved by the GCMs. Despite these biases, our simulations successfully reproduce the observed Arctic $\delta^{18}O_p$ variation in response to the prescribed sea-ice conditions, which enables us to investigate how sea-ice changes affect Arctic $\delta^{18}O_p$.

Changes in Arctic sea ice and precipitation $\delta^{18}O$

Both summer (JJA) and winter (DJF) have exhibited a rapid decline in sea ice over the period 1979–2020 (Fig. 2a, b), but they are not spatially uniform. The decline in summer is more widespread, with the strongest decline mainly occurring in the western Arctic including the Beaufort, Chukchi and East Siberian seas (Xia et al. 2014; Liu et al. 2021) and the BKS, featuring an average decline >6.20% per decade (Fig. 2a, Supplementary Fig. S1). By contrast, winter sea-ice decline is somewhat weaker in both magnitude and spatial extent. The strongest decline is mainly located in the BKS (Liu et al.

Citation: *Polar Research* 2023, *42*, 9751, http://dx.doi.org/10.33265/polar.v42.9751

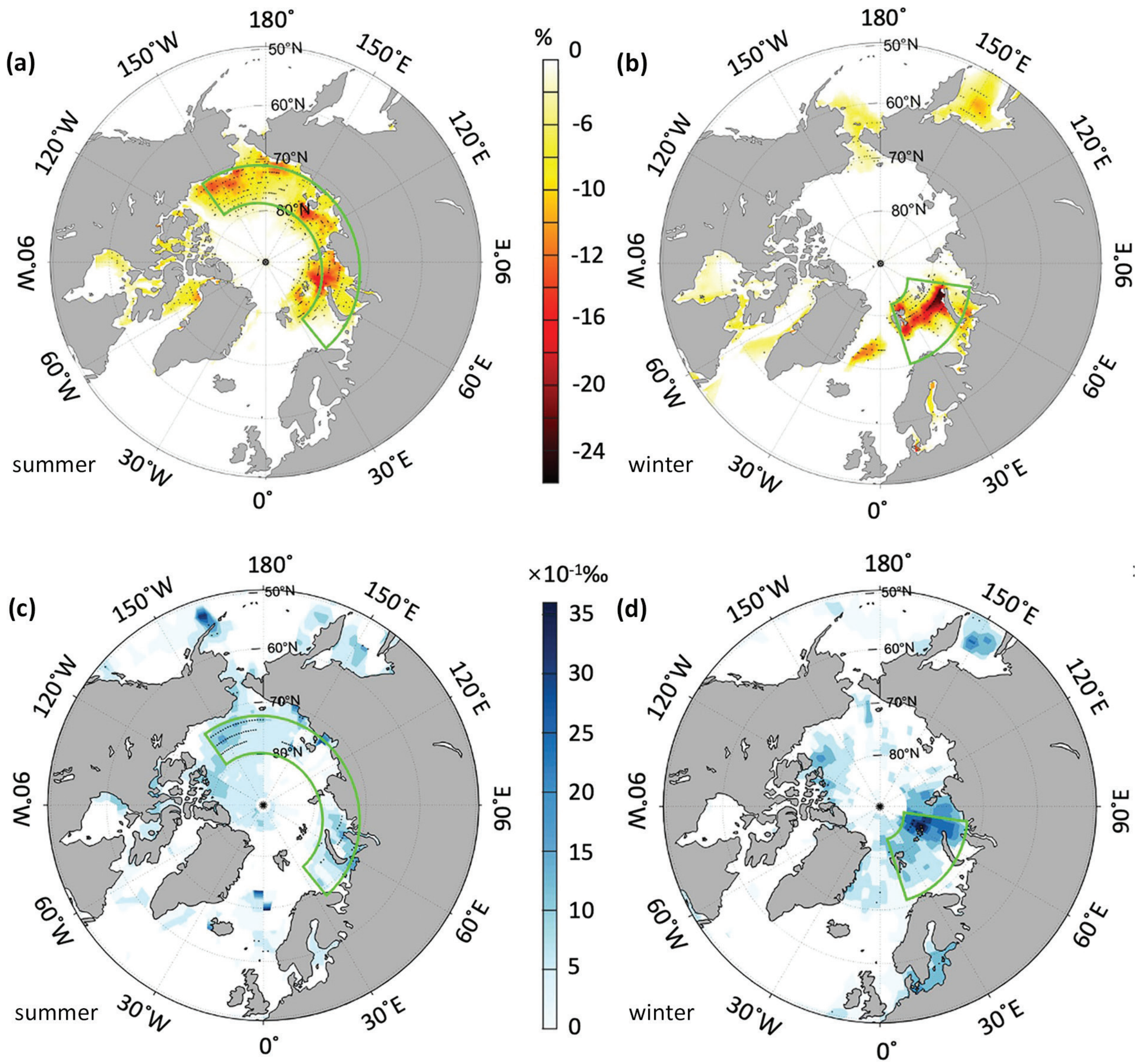

Fig. 2 Linear trend of observed Arctic (a) summer (JJA) and (b) winter (DJF) SIC (% per decade) during the period 1979–2020. Simulated Arctic precipitation $\delta^{18}O$ ($\delta^{18}O_p$) in (c) summer and (d) winter (‰ per decade). Green outlines show the area with the strongest sea-ice decline (35–215°E and 71–76°N for JJA and 20–80°E and 70–85°N for DJF). The stippling indicates statistical significance at the 5% confidence level.

2022), where the SIC has been decreasing at a rate of approximately 5.10% per decade (Fig. 2b, Supplementary Fig. S1). The rapid sea-ice reduction not only amplifies Arctic warming (Screen & Simmonds 2010) but also intensifies local evaporation (Bintanja & Selten 2014; Allan et al. 2020). These coherent changes in temperature and local evaporation due to sea-ice loss may have left an isotopic imprint in Arctic precipitation, reflected in enrichment of $\delta^{18}O_p$.

We calculated the linear trends of simulated Arctic summer and winter $\delta^{18}O_p$ over the period 1979–2020 (Fig. 2c, d). Concomitant with the trends in sea ice are obvious changes in Arctic $\delta^{18}O_p$: both seasons show distinct spatial patterns, with increased trends largely occurring in the regions of strong sea-ice reduction (Fig. 2a, b). During the summer season, a significant rising trend in $\delta^{18}O_p$ is observed in the western Arctic and the BKS, where $d^{18}O_p$ increases at an average rate of 0.52‰/decade (Fig. 2c). The increase in winter $\delta^{18}O_p$ appears more rapid, with the largest increase taking place in the BKS, where $\delta^{18}O_p$ has an average trend of 0.98‰/decade (Fig. 2d).

Correlations between Arctic precipitation $\delta^{18}O$, sea ice and local temperature

To further explore the potential influence of seasonal sea-ice loss on Arctic $\delta^{18}O_p$, we constructed the time series of SIC, air temperature and $\delta^{18}O_p$ (Figs. 3, 4) by averaging these fields over the regions with the strongest sea-ice declines (Fig. 2). The observed SIC shows significant correlations with simulated $\delta^{18}O_p$ in both summer and winter (Fig. 3a, b). During summer, Arctic $\delta^{18}O_p$ is negatively correlated with SIC, with a simultaneous correlation of −0.40 and a maximum correlation of −0.82 when SIC leads $\delta^{18}O_p$ by two months (Fig. 3a). This lagged response of $\delta^{18}O_p$ to sea-ice loss is also reflected in the response of $\delta^{18}O_p$ to temperature (Fig. 3c), but the associated mechanisms remain unclear. Considering strong summer sea-ice loss, we suggest that these delayed $\delta^{18}O_p$ responses probably reflect the influence of local evaporation on Arctic precipitation and its $\delta^{18}O_p$. Warming and evaporation caused by sea-ice loss in summer can persist into autumn and winter (Fig. 3a, c) through sea-ice–air feedbacks (Holland et al. 2010; Stroeve et al. 2012), which in turn affect precipitation and its $\delta^{18}O_p$. The observed summer SIC index for the period 1979–2020 shows a significant decrease superimposed on strong interannual-to-decadal variability (Fig. 4a). The SIC tended to decline slowly until 2000, and since then, the decline has accelerated, culminating in a record low in 2019. These changes in summer sea ice are largely in parallel with the evolution of simulated $\delta^{18}O_p$ index, which shows an apparent upward trend (Fig. 4a). These coherences between summer sea-ice and $\delta^{18}O_p$ changes suggest that the rapid sea-ice loss has led to enriched Arctic $\delta^{18}O_p$, probably through amplified warming or local evaporation, or both.

By contrast, winter SIC exhibits a relatively weak declining trend, but with stronger interannual and decadal fluctuations (Fig. 4b). A rapid decline was observed after the mid-2000s, with a record low SIC in winter 2017. These changes in the SIC index are also mirrored by simulated winter $\delta^{18}O_p$ index, and they show a significant negative correlation, with the strongest correlation (r = −0.88) for a zero Lag (Figs. 3b, 4b). These links between the indices of SIC and $\delta^{18}O_p$ are still robust even after the linear trends are removed (Fig. 5a, b). Robust linkages between SIC and $\delta^{18}O_p$ suggest that the rapid sea-ice loss may have a strong isotopic imprint in Arctic precipitation, but with the strongest signal being synchronous for winter and two-month lagged for summer.

Considering the strong temperature effect on $\delta^{18}O_p$ at high latitudes (Dansgaard 1964), we also explore the influence of warming on Arctic $\delta^{18}O_p$ in the model. The calculated long-term changes of Arctic temperature and $\delta^{18}O_p$ generally reveal the strong temporal coherence, with the strongest correlations when the temperature leads the $\delta^{18}O_p$ by two months for summer (r = 0.66) and by 0 months for winter (r = 0.92; Fig. 3c, d). The correlations become weak but are still robust when the linear trends are removed for the data (Fig. 5c, d). These are consistent with the above-mentioned SIC correlations (Figs. 3, 4). The Arctic temperature shows an apparent

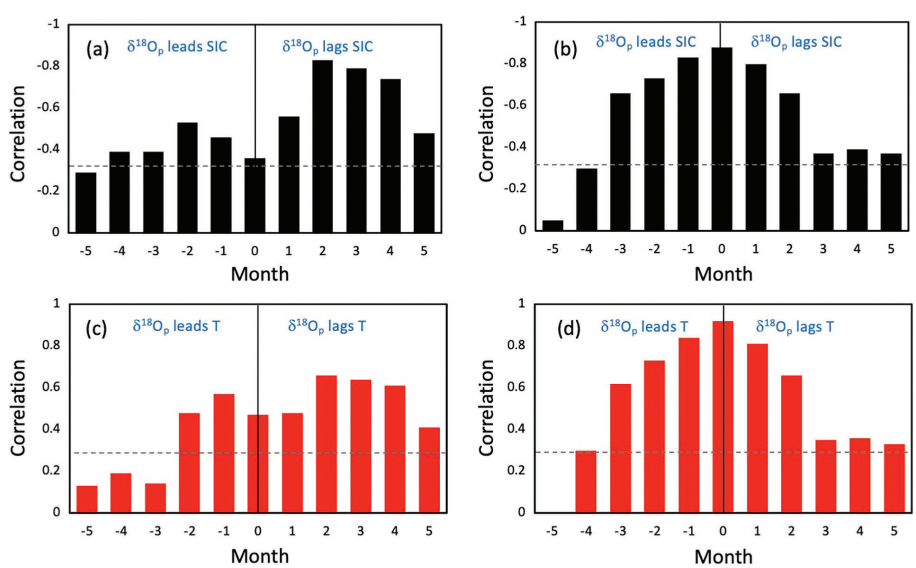

Fig. 3 Lead-lag correlations between $\delta^{18}O_p$ and SIC time series (averaged over the area with the strongest sea-ice decline shown in Fig. 2 in (a) summer and (b) winter during the period 1979–2020). Lead-lag correlations between temperature and $\delta^{18}O_p$ in (c) summer and (d) winter. Positive lag indicates that the SIC or temperature is leading the $\delta^{18}O_p$. Dashed line indicates the 5% significance level.

Citation: *Polar Research* 2023, *42*, 9751, http://dx.doi.org/10.33265/polar.v42.9751

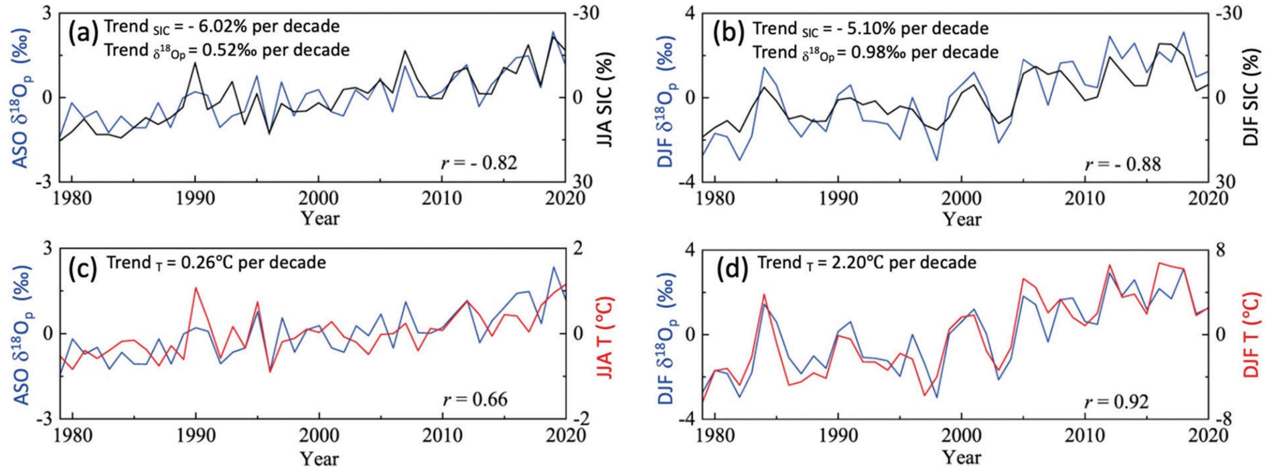

Fig. 4 (a) Time series of summer (JJA) SIC (black) and autumn (ASO) $\delta^{18}O_p$ (blue) anomalies. (b) Time series of winter (DJF) SIC (black) and $\delta^{18}O_p$ (blue) anomalies. Time series of (c) summer and (d) winter $\delta^{18}O_p$ (blue) anomalies for temperature (red) and $\delta^{18}O_p$. The two seasons for the $\delta^{18}O_p$ were chosen based on the maximum correlation between SIC and $\delta^{18}O_p$ (see Fig. 3).

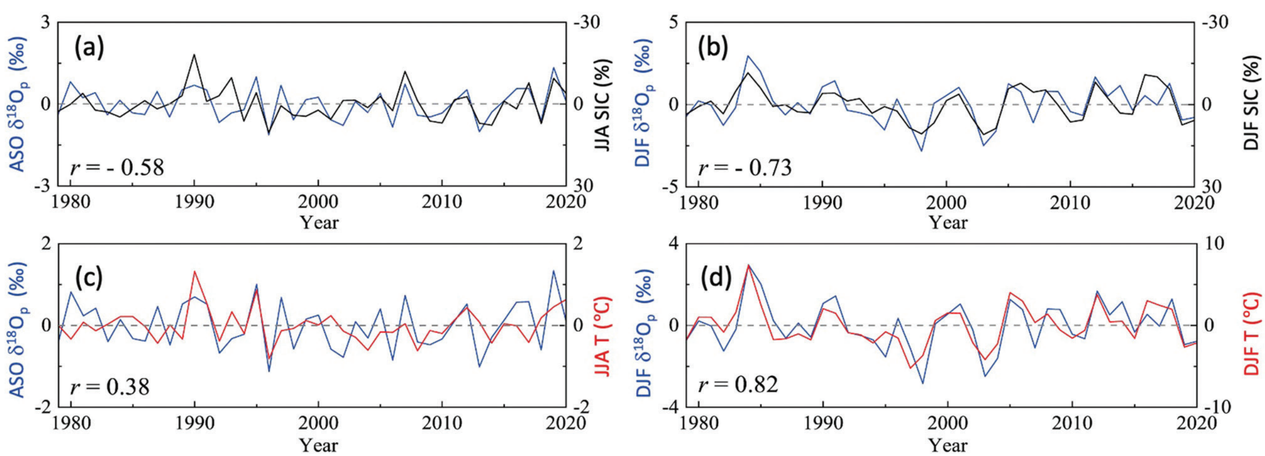

Fig. 5 (a) Detrended time series of summer (JJA) SIC (black) and autumn (ASO) $\delta^{18}O_p$ (blue) anomalies. (b) Detrended time series of winter (DJF) SIC (black) and $\delta^{18}O_p$ (blue) anomalies. Detrended time series of (c) summer and (d) winter $\delta^{18}O_p$ (blue) anomalies for temperature (red) and $\delta^{18}O_p$

warming over the study period, with the rates of 0.26 °C/decade for summer and 2.2 °C/decade for winter (Fig. 4c, d). These warming trends are consistent with those (0.5 and 2.1 °C/decade) reported by Screen & Simmonds (2010) but with a slight over- or underestimation. The biases arise largely from a different calculation procedure adopted by Screen & Simmonds (2010) who focused on air temperature of the 950–1000-hPa layer over the whole Arctic (70–90°N). The trends and variability in Arctic warming are also mirrored in the corresponding Arctic $\delta^{18}O_p$, especially during winter season when Arctic warming is strongest (Screen & Simmonds 2010). Given these robust linkages and the well-documented temperature effect on $\delta^{18}O_p$ at high latitudes, the rapid Arctic warming may have contributed to Arctic $\delta^{18}O_p$ enrichment. The calculated temperature slope coefficients are 1.11‰/°C for summer and 0.41‰/°C for winter (Fig. 6), which are largely within the range of 0.25–1.10‰/°C reported by Rozanski et al. (1993) and Bowen (2008) and compare well with the observed annual mean slopes in Greenland (0.67‰/°C) by Johnsen et al. (1989) and in the whole Arctic slope (0.38–0.53‰/°C) by Faber et al. (2017). The seasonal difference in temperature slope coefficient has been attributed to the seasonal variability in temperature, moisture sources and precipitation (Bowen 2008) and condensation temperatures (Kohn & Welker 2005).

Significant correlations of Arctic $\delta^{18}O_p$ with SIC and local temperature indicate that both sea ice and temperature act as drivers of changes in Arctic $\delta^{18}O_p$. However, the strength of these correlations varies between seasons. In contrast to the winter season, when Arctic $\delta^{18}O_p$ is

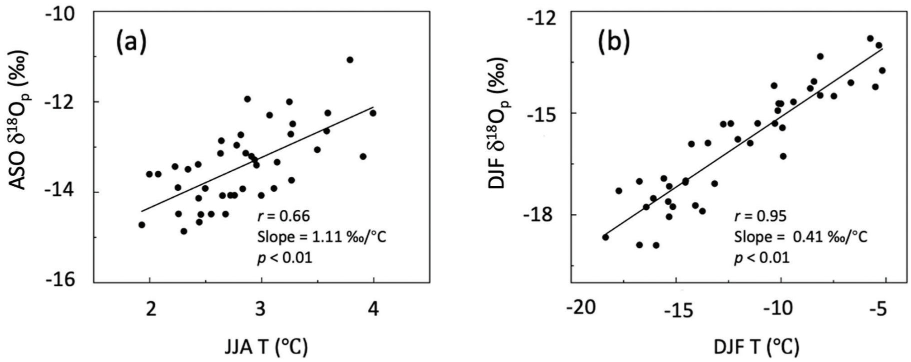

Fig. 6 (a) Summer (JJA) and (b) winter (DJF) plotted against ASO $\delta^{18}O_p$ during the period 1979–2020. The two seasons for the $\delta^{18}O_p$ are chosen based on the maximum correlation between temperature and $\delta^{18}O_p$ (see Fig. 3).

strongly correlated with both SIC and temperature, the summer temperature-$\delta^{18}O_p$ correlation is weaker and is even lower than the SIC-$\delta^{18}O_p$ correlation. These suggest that changes in Arctic $\delta^{18}O_p$ are likely to be a result of a combination of local temperature and evaporation due to sea-ice loss, but the relative importance of these processes is season dependent.

Discussion

Sea-ice loss affects Arctic precipitation δ18O: temperature effect

Our results demonstrate that variability and changes in Arctic $\delta^{18}O_p$ arise largely from a combined effect of sea ice and local temperature (Figs. 4, 5). The apparent tendency towards more enriched Arctic $\delta^{18}O_p$ is coincident with Arctic warming, which is easy to understand in terms of temperature-dependent isotopic fractionation (Dansgaard 1964). However, isolating the impact of local temperature from sea-ice loss is challenging because of strong coupling between local temperature and sea-ice melt. Previous studies have suggested that sea-ice loss plays a leading role in recent Arctic warming through ice-temperature feedbacks (Screen & Simmonds 2010; Overland et al. 2011; Stuecker et al. 2018; Dai et al. 2019). The linkage between Arctic $\delta^{18}O_p$ and temperature may reflect the influence of sea-ice loss associated warming on local $\delta^{18}O_p$. The rapid sea-ice decline enhances heat flux from the ocean to atmosphere, leading to lower-level atmospheric warming (Screen & Simmonds 2010), leading to enriched Arctic $\delta^{18}O_p$. The simulated Arctic summer warming has a trend of 0.26 °C/decade over the period 1979–2020 (a total of 1.09 °C), implying an enrichment of 1.21‰ in $\delta^{18}O_p$ (according to summer temperature slope coefficients of 1.11‰/°C; Fig. 6), which accounts for 55% of change in simulated Arctic $\delta^{18}O_p$ (an increase of 2.18‰, according to summer $\delta^{18}O_p$ slope of 0.52‰/decade). This difference probably reflects the influence of other processes such as moisture sources that can alter the Arctic $\delta^{18}O_p$ and thus affect the temperature–$\delta^{18}O_p$ relationship (Hendricks et al. 2000; Faber et al. 2017). By contrast, the simulated Arctic winter warming is much faster (2.20 °C/decade) and yields a corresponding enrichment in $\delta^{18}O_p$ by 3.79‰, contributing about 92% (Fig. 6) to the change in simulated Arctic $\delta^{18}O_p$. This contrasting temperature effect between seasons is in accord with Arctic warming, which is strongest in winter and weakest in summer (Screen & Simmonds 2010).

Sea-ice loss affects Arctic precipitation δ18O: local evaporation

As discussed earlier, moisture dynamics is also potentially an important driver of changes in Arctic $\delta^{18}O_p$, especially during the summer. The rapid sea-ice loss can cause an increase in Arctic water vapour through not only enhanced local evaporation (Bintanja & Selten 2014; Bintanja & Andry 2017) but also increased poleward moisture transport (Graversen et al. 2008; Screen & Simmonds 2012). However, the influence of these processes on Arctic $\delta^{18}O_p$ is still a matter of debate. A recent study by Mellat et al. (2021) using observational data from one summer season found that sea-ice loss tends to produce more depleted Arctic $\delta^{18}O_p$ due to enhanced local evaporation, but this contradicts the results from both simulations (Faber et al. 2017) and observations (Klein et al. 2015; Putman et al. 2017). These latter studies suggested that Arctic precipitation derived from advected moisture generally has more depleted $\delta^{18}O_p$ compared to that derived from local evaporation on the account of the longer distillation pathway of storms travelling from lower-latitude source to the Arctic.

To further determine how seasonal sea-ice loss affects Arctic $\delta^{18}O_p$ through moisture dynamics, we used the

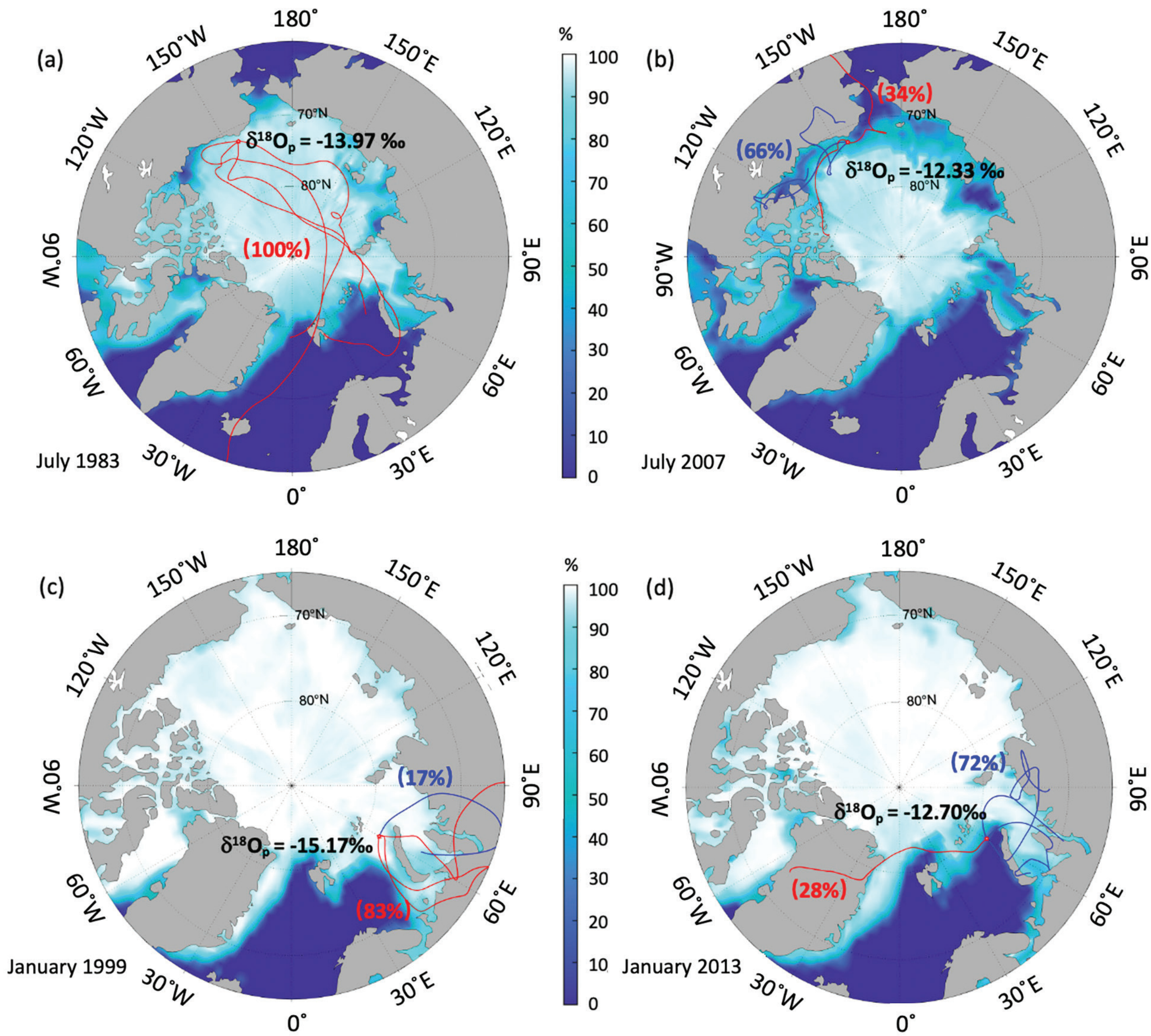

Fig. 7 Back trajectory clusters (red lines represent the remote part, whilst blue lines represent the local part) calculated from every six-hour trajectory with a pathway of 15 days at a selected site (72°N, 155°W) in the western Arctic that have (a) a maximum (July 1983) and (b) a minimum (July 2007) SIC (colour bar); $\delta^{18}O_p$ values are indicated in black. A seven-day pathway at a selected site (78°N, 60°E) in the BKS for (c) January of 1999 (with maximum SIC) and (d) 2013 (with minimum SIC).

HYSPLIT model to investigate moisture source changes and associated $\delta^{18}O_p$ behaviours for extreme sea-ice conditions (Fig. 7). In the western Arctic, where summer melt is strongest over the study period, we compare moisture trajectories and $\delta^{18}O_p$ values between July 1983 and July 2007, the months that have maximum (July 1983) and minimum (July 2007) sea-ice extent, respectively (Fig. 7a, b). During the summer of 1983, the BS was covered by ice and received precipitation from North Atlantic-sourced moisture that passed through the North Pole before arriving at the region. The long-distance transport of moisture was associated with a stronger rain-out process and led to more depleted $\delta^{18}O_p$ (Fig. 7a). By contrast, the BS and adjacent seas were largely ice-free during the summer of 2007 and received moisture from the western Arctic Ocean. This proximity of moisture source probably reflected the contribution of local evaporation due to sea-ice loss and was characterized by more enriched $\delta^{18}O_p$ (Fig. 7b). This also holds true for winter, during which sea-ice melt is relatively weak and is concentrated in the BKS (Fig. 7c, d). In contrast, the winter of 1999 that was characterized by more depleted $\delta^{18}O_p$ in the BKS due to large contribution from external moisture (Fig. 7c), lower SIC in the BKS during the winter of 2013 contributed to more local moisture through evaporation and yielded more enriched $\delta^{18}O_p$ in the region (Fig. 7d). Our trajectory analysis further corroborates that local evaporation due to sea-ice loss is an important driver of Arctic summer $\delta^{18}O_p$ enrichment in summer, but this influence is very limited during winter. This is not surprising because rapid sea-ice reduction and higher temperature during summer strongly enhance local evaporation.

Although our trajectory analysis provides an insight into the influence of dynamics on the link between sea-ice loss and Arctic $\delta^{18}O_p$, there are some caveats worth noting. First, we calculated the trajectories based only on the individual months with maximum and minimum sea-ice coverage, which may not represent the climatological trajectories due to sea-ice changes. Second, the trajectories themselves do not provide mechanistic evidence for the effects of locally evaporated and advected moisture impact on Arctic $\delta^{18}O_p$. Therefore, further analysis—using backward trajectories or moisture tagging tools—is needed to better understand the influence of moisture dynamics due to sea-ice loss on Arctic $\delta^{18}O_p$.

Our results are consistent with previous observations (Klein et al. 2015; Putman et al. 2017) and simulations (Faber et al. 2017) in suggesting that sea-ice loss enriches Arctic $\delta^{18}O_p$, but they reveal a substantial seasonal difference that contrasts with previous work. We also note that our results contradict the recent observational study that suggested more depleted Arctic $\delta^{18}O_p$ in response to local evaporation due to sea-ice loss (Mellat et al. 2021). This disagreement likely arises from the fact that the findings of Mellat et al. (2021) are based exclusively on land stations that may not fully represent the oceanic regions where sea-ice loss occurs, in addition to event-scale sampling (within one summer) that may not reflect the response of $\delta^{18}O_p$ to local evaporation due to the delayed influence of sea-ice loss on Arctic precipitation.

Implications for Arctic hydroclimate studies

An improved understanding of how sea-ice changes affect Arctic precipitation isotope ratios can offer a number of opportunities for studying the modern Arctic hydrological cycle. The Arctic is currently undergoing rapid changes, characterized by amplified warming and dramatic sea-ice loss, both of which have contributed to increased local evaporation and precipitation (Vihma et al. 2016; Ford & Frauenfeld 2022). These hydrological changes have been modelled extensively (Bintanja & Selten 2014; Ford & Frauenfeld 2022), but the absence of direct hydrological measurements makes them very difficult to verify observationally. In particular, disentangling the relative importance of local and remote moisture in Arctic precipitation is still under debate. Our work highlights the potential of using stable water isotopes to investigate Arctic sea-ice changes and associated moisture dynamics. The distinct isotopic signals of local and remote moisture identified here represent a simple method that could be applied to gain first-order information on the moisture dynamics of Arctic precipitation.

Within the palaeoclimate field, isotopic archives from polar ice core have been widely used for the reconstruction of palaeotemperature, but an accurate reconstruction depends on reliable modern temperature/$\delta^{18}O_p$ relationships. Previous studies have demonstrated that reconstruction of palaeotemperature using generalized temperature/$\delta^{18}O_p$ response functions may be a problematic method because the temperature/$\delta^{18}O_p$ relationship may not be constant in time (Hendricks et al. 2000; Holme et al. 2019). The results presented here suggest that enhanced local evaporation due to Arctic ice loss or sublimation of snow/sea ice in warm climates (i.e., interglacial times) can lead to more enriched Arctic $\delta^{18}O_p$, which can alter the temperature–$\delta^{18}O$ relationships (Hendricks et al. 2000) and may thereby result in large errors in palaeotemperature reconstructions. Our study emphasizes that the inversion of generalized temperature/$\delta^{18}O_p$ relationship functions represents a limited method for palaeotemperature reconstructions, and the use of this method must be treated with caution (Bowen 2008).

Conclusions

In this study, we quantify the influence of sea-ice loss on Arctic precipitation isotope ratios using an atmospheric GCM equipped with explicit water isotope diagnostics. Our simulations successfully capture observed spatial and temporal behaviours of Arctic temperature and $\delta^{18}O_p$. The simulated Arctic precipitation shows an apparent isotopic enrichment in response to sea-ice reduction in both summer and winter seasons. This characteristic isotopic imprint of sea-ice changes is a combined effect of Arctic warming and local evaporation due to sea-ice loss. However, the relative influence of the two processes on Arctic $\delta^{18}O_p$ differs strongly between seasons. During summer, enhanced local evaporation and warmer temperature contribute approximately equally to Arctic $\delta^{18}O_p$ enrichment. By contrast, changes in Arctic winter $\delta^{18}O_p$ are predominantly controlled by local temperature. These results support the conclusions of Faber et al. (2017) that decreased (increased) sea ice yields more enriched (depleted) Arctic $\delta^{18}O_p$ but reveal substantial seasonal difference in the driving mechanisms that contrasts the previous work. Our work highlights the importance of local evaporation due to sea-ice loss in determining Arctic $\delta^{18}O_p$ and the temperature/$\delta^{18}O_p$ relationships and may

Citation: *Polar Research* 2023, *42*, 9751, http://dx.doi.org/10.33265/polar.v42.9751

have implications for the hydrological cycle and palaeotemperature reconstructions in the Arctic.

Acknowledgements

The authors acknowledge the Air Resources Laboratory, National Oceanic and Atmospheric Administration, for providing the HYSPLIT transport model. SIC data were obtained from the NSIDC (available at https://nsidc.org/data/G02202/versions/4). Observed precipitation $\delta^{18}O$ data at Arctic stations were obtained from the GNIP data set (https://nucleus.iaea.org/wiser/index.aspx).

Disclosure statement

The authors declare no conflicts of interest.

Funding

This work was supported by the National Natural Science Foundation of China (grant nos. 42025602 and 41876039).

References

Adler R.F., Huffman G.J., Chang A., Ferraro R., Xie P.P., Janowiak J., Rudolf B., Schneider U., Curtis S., Bolvin D., Gruber A., Susskind J., Arkin P. & Nelkin E. 2003. The version-2 Global Precipitation Climatology Project (GPCP) monthly precipitation analysis (1979-present). *Journal of Hydrometeorology 4*, 1147–1167, doi: 10.1175/1525-7541.

Allan R.P., Barlow M., Byrne M.P., Cherchi A., Douville H., Fowler H.J., Gan T.Y., Pendergrass A.G., Rosenfeld D., Swann A.L., Wilcox L.J. & Zolina O. 2020. Advances in understanding large-scale responses of the water cycle to climate change. *Annals of the New York Academy of Sciences 1472*, 49–75, doi: 10.1111/nyas.14337.

Bailey H., Hubbard A., Klein E.S., Mustonen K.R., Akers P.D., Marttila H. & Welker J.M. 2021. Arctic sea-ice loss fuels extreme European snowfall. *Nature Geoscience 14*, 283–288, doi: 10.1038/s41561-021-00719-y.

Bintanja R. & Andry O. 2017. Towards a rain-dominated Arctic. *Nature Climate Change 7*, 263–267, doi: 10.1038/nclimate3240.

Bintanja R. & Selten F.M. 2014. Future increases in Arctic precipitation linked to local evaporation and sea-ice retreat. *Nature 509*, 479–482, doi: 10.1038/nature13259.

Blunden J. & Arndt D.S. 2012. *State of the climate in 2011. Bulletin of the American Meteorological Society 93*, S1–S264, doi: 10.1175/2012BAMSStateoftheClimate.1.

Boisvert L.N., Webster M.A., Petty A.A., Markus T., Bromwich D.H. & Cullather R.I. 2018. Intercomparison of precipitation estimates over the Arctic Ocean and its peripheral seas from reanalyses. *Journal of Climate 31*, 8441–8462, doi: 10.1175/JCLI-D-18-0125.1.

Bonne J.L., Masson-Delmotte V., Cattani O., Delmotte M., Risi C., Sodemann H. & Steen-Larsen H.C. 2014. The isotopic composition of water vapour and precipitation in Ivittuut, southern Greenland. *Atmospheric Chemistry and Physics 14*, 4419–4439, doi: 10.5194/acp-14-4419-2014.

Bowen G.J. 2008. Spatial analysis of the intra-annual variation of precipitation isotope ratios and its climatological corollaries. *Journal of Geophysical Research—Atmospheres 113*, article no. D05113, doi: 10.1029/2007JD009295.

Bowen G.J., Cai Z., Fiorella R.P. & Putman A.L. 2019. Isotopes in the water cycle: regional-to global-scale patterns and applications. *Annual Review of Earth and Planetary Sciences 47*, 453–479, doi: 10.1146/annurev-earth-053018-060220.

Cluett A., Thomas E., Evans S. & Keys P. 2021. Seasonal variations in moisture origin explain spatial contrast in precipitation isotope seasonality on coastal western Greenland. *Journal of Geophysical Research—Atmospheres 126*, e2020JD033543, doi: 10.1029/2020JD033543.

Cohen J., Screen J.A., Furtado J.C., Barlow M., Whittleston D., Coumou D., Francis J., Dethloff K., Entekhabi D., Overland J. & Jones J. 2014. Recent Arctic amplification and extreme mid-latitude weather. *Nature Geoscience 7*, 627–637, doi: 10.1038/ngeo2234.

Dai A., Luo D., Song M. & Liu J. 2019. Arctic amplification is caused by sea-ice loss under increasing CO_2. *Nature Communications 10*, article no. 121, doi: 10.1038/s41467-018-07954-9.

Dansgaard W. 1964. Stable isotopes in precipitation. *Tellus 16*, 436–468, doi: 10.3402/tellusa.v16i4.8993.

Draxler R.R. & Hess G. 1998. An overview of the HYSPLIT_4 modelling system for trajectories, dispersion, and deposition. *Australian Meteorological Magazine 47*, 295–308.

Faber A.K., Møllesøe Vinther B., Sjolte J. & Anker Pedersen R. 2017. How does sea ice influence $\delta^{18}O$ of Arctic precipitation? *Atmospheric Chemistry and Physics 17*, 5865–5876, doi: 10.5194/acp-17-5865-2017.

Ford V.L. & Frauenfeld O.W. 2022. Arctic precipitation recycling and hydrologic budget changes in response to sea ice loss. *Global and Planetary Change 209*, article no. 103752, doi: 10.1016/j.gloplacha.2022.103752.

Fröhlich K., Gibson J.J. & Aggarwal P.K. 2002. Deuterium excess in precipitation and its climatological significance. IAEA-CN-80/104. In: *Proceedings. Study of environmental change using isotope techniques. C & S Papers Series 13/P*. Pp. 54–66. Vienna: International Atomic Energy Agency.

Galewsky J., Steen-Larsen H.C., Field R.D., Worden J., Risi C. & Schneider M. 2016. Stable isotopes in atmospheric water vapor and applications to the hydrologic cycle. *Reviews of Geophysics 54*, 809–865, doi: 10.1002/2015rg000512.

Gat J.R., Bowser C.J. & Kendall C. 1994. The contribution of evaporation from the Great Lakes to the continental atmosphere: estimate based on stable isotope data. *Geophysical Research Letters 21*, 557–560, doi: 10.1029/94GL00069.

Graversen R.G., Mauritsen T., Tjernström M., Källén E. & Svensson G. 2008. Vertical structure of recent Arctic warming. *Nature 451*, 53–56, doi: 10.1038/nature06502.

Hendricks M., DePaolo D. & Cohen R. 2000. Space and time variation of $\delta^{18}O$ and δD in precipitation: can paleotemperature be estimated from ice cores? *Global Biogeochemical Cycles 14*, 851–861, doi: 10.1029/1999GB001198.

Holland M.M., Serreze M.C. & Stroeve J. 2010. The sea ice mass budget of the Arctic and its future change as simulated by coupled climate models. *Climate Dynamics 34*, 185–200, doi: 10.1007/s00382-008-0493-4.

Holme C., Gkinis V., Lanzky M., Morris V., Olesen M., Thayer A., Vaughn B.H. & Vinther B.M. 2019. Varying regional δ^{18}O-temperature relationship in high-resolution stable water isotopes from east Greenland, *Climate of the Past 15*, 893–912, doi: 10.5194/cp-15-893-2019.

Huang Y., Dong X., Bailey D.A., Holland M.M., Xi B., DuVivier A.K., Kay J.E., Landrum L.L. & Deng Y. 2019. Thicker clouds and accelerated Arctic sea ice decline: the atmosphere–sea ice interactions in spring. *Geophysical Research Letters 46*, 6980–6989, doi: 10.1029/2019GL082791.

IAEA/WMO [International Atomic Energy Agency/World Meterological Organization] 2019. Global Network of Isotopes in Precipitation. Database accessed on the internet at https://www.iaea.org/services/networks/gnip on 20 May 2022.

Johnsen S.J., Dansgaard W. & White J.W.C. 1989. The origin of Arctic precipitation under present and glacial conditions. *Tellus B 41*, 452–468, doi: 10.3402/tellusb.v41i4.15100.

Jouzel J., Alley R.B., Cuffey K.M., Dansgaard W., Grootes P., Hoffmann G., Johnsen S.J., Koster R.D., Peel D., Shuman S.A., Stievenard M., Stuiver M. & White J. 1997. Validity of the temperature reconstruction from water isotopes in ice cores. *Journal of Geophysical Research—Oceans 102*, 26471–26487, doi: 10.1029/97JC01283.

Kanamitsu M., Ebisuzaki W., Woollen J., Yang S.K., Hnilo J.J., Fiorino M. & Potter G.L. 2002. NCEP–DOE AMIP-II Reanalysis (R-2). *Bulletin of the American Meteorological Society 83*, 1631–1644, doi: 10.1175/bams-83-11-1631.

Klein E.S., Cherry J., Young J., Noone D., Leffler A. & Welker J.J.S. 2015. Arctic cyclone water vapor isotopes support past sea ice retreat recorded in Greenland ice. *Scientific Report 5*, article no. 10295, doi: 10.1038/srep10295.

Klein E.S. & Welker J.M. 2016. Influence of sea ice on ocean water vapor isotopes and Greenland ice core records. *Geophysical Research Letters 43*, 12475–12483, doi: 10.1002/2016gl071748.

Kohn M.J. & Welker J.M. 2005. On the temperature correlation of δ^{18}O in modern precipitation. *Earth and Planetary Science Letters 231*, 87–96, doi: 10.1016/j.epsl.2004.12.004.

Kopec B.G., Feng X., Michel F.A. & Posmentier E.S. 2016. Influence of sea ice on Arctic precipitation. *Proceedings of the National Academy Sciences of the United States of America 113*, 46–51, doi: 10.1073/pnas.1504633113.

Kurita N. 2011. Origin of Arctic water vapor during the ice-growth season. *Geophysical Research Letters 38*, 35–43, doi: 10.1029/2010gl046064.

Leroy-dos Santos C., Masson-Delmotte V., Casado M., Fourré E., Steen-Larsen H., Maturilli M., Orsi A., Berchet A., Cattani O., Minster B., Gherardi J. & Landais A. 2020. A 4.5 year-long record of Svalbard water vapor isotopic composition documents winter air mass origin. *Journal of Geophysical Research—Atmosphere 125*, article no. 32681, doi: 10.1029/2020JD032681.

Liu Z., Risi C., Codron F., He X., Poulsen C.J., Wei Z., Chen D., Li S. & Bowen G.J. 2021. Acceleration of western Arctic sea ice loss linked to the Pacific North American pattern. *Nature Communication 12*, article no. 1519, doi: 10.1038/s41467-021-21830-z.

Liu Z., Risi C., Codron F., Jian Z., Wei Z., He X., Poulsen C.J., Wang Y., Chen D., Ma W., Cheng Y. & Bowen G.J. 2022. Atmospheric forcing dominates winter Barents–Kara sea ice variability on interannual to decadal time scales. *Procceedings of the National Academy Sciences of the United States of America 119*, e2120770119, doi: 10.1073/pnas.2120770119.

Liu Z., Yoshimura K., Bowen G.J. & Welker J.M. 2014. Pacific–North American teleconnection controls on precipitation isotopes (δ^{18}O) across the contiguous United States and adjacent regions: a GCM-based analysis. *Journal of Climate 27*, 1046–1061, doi: 10.1175/JCLI-D-13-00334.1.

Meier W.N., Fetterer F.A., Windnagel K. & Stewart J.S. 2021. *NOAA/NSIDC Climate Data Record of Passive Microwave Sea Ice Concentration, version 4*. Data set id G02202, doi: 10.7265/efmz-2t65. Boulder, CO: National Snow and Ice Data Center. Accessed on the internet at https://nsidc.org/data/g02202/versions/4 on 16 May 2023.

Mellat M., Bailey H., Mustonen K.R., Marttila H., Klein E.S., Gribanov K., Bret-Harte M.S., Chupakov A.V., Divine D.V., Else B., Filippov L., Hyöky V., Jones S., Kirpotin S.N., Kroon A., Markussen H.T., Nielsen M., Olsen M., Paavola R., Pokrovsky O.S., Prokushkin A., Rasch M., Raundrup K., Suominen O., Syvänperä L., Vignisson S.R., Zarov E. & Welker J.M. 2021. Hydroclimatic controls on the isotopic (δ^{18}O, δ^{2}H, d-excess) traits of pan-Arctic summer rainfall events. *Frontiers in Earth Science 367*, 45–60, doi: 10.3389/feart.2021.651731.

Merlivat L. & Jouzel J. 1979. Global climatic interpretation of the deuterium-oxygen 18 relationship for precipitation. *Journal of Geophysical Research—Oceans 84*, 5029–5033, doi: 10.1029/JC084iC08p05029.

Nan Y., He Z., Tian F., Wei Z. & Tian L. 2021. Can we use precipitation isotope outputs of isotopic general circulation models to improve hydrological modeling in large mountainous catchments on the Tibetan Plateau? *Hydrology and Earth System Sciences 25*, 6151–6172, doi: 10.5194/hess-25-6151-2021.

Overland J.E. & Wang M. 2013. When will the summer Arctic be nearly sea ice free? *Geophysical Research Letters 40*, 2097–2101, doi: 10.1002/grl.50316.

Overland J.E., Wood K.R. & Wang M. 2011. Warm Arctic-cold continents: climate impacts of the newly open Arctic Sea. *Polar Research 30*, 567–570, doi: 10.3402/polar.v30i0.15787.

Puntsag T., Mitchell M.J., Campbell J.L., Klein E.S., Likens G.E. & Welker J.M. 2016. Arctic Vortex changes alter the sources and isotopic values of precipitation in northeastern US. *Scientific Reports 6*, article no. 22647, doi: 10.1038/srep22647.

Putman A.L., Feng X., Sonder L.J. & Posmentier E.S. 2017. Annual variation in event-scale precipitation δ^{2}H at Barrow, AK, reflects vapor source region. *Atmospheric Chemistry and Physics 17*, 4627–4639, doi: 10.5194/acp-17-4627-2017.

Reynolds R.W., Smith T.M., Liu C., Chelton D.B., Casey K.S. & Schlax M.G. 2007. Daily high-resolution-blended analyses for sea surface temperature. *Journal of Climate 20*, 5473–5496, doi: 10.1175/2007JCLI1824.1.

Rozanski K., Araguás-Araguás L. & Gonfiantini R. 1993. Isotopic patterns in modern global precipitation. In P.K. Swart et al. (eds.): *Climate change in continental isotopic records. Geophysical Monograph Series 78*. Pp. 1–36. Washington, DC: American Geophysical Union.

Screen J.A. & Simmonds I. 2010. The central role of diminishing sea ice in recent Arctic temperature amplification. *Nature 464*, 1334–1337, doi: 10.1038/nature09051.

Screen J.A. & Simmonds I. 2012. Declining summer snowfall in the Arctic: causes, impacts and feedbacks. *Climate Dynamics 38*, 2243–2256, doi: 10.1007/s00382-011-1105-2.

Sime L.C., Hopcroft P.O. & Rhodes R.H. 2019. Impact of abrupt sea ice loss on Greenland water isotopes during the last glacial period. *Proceedings of the National Academy of Sciences of the United States of America 116*, 4099–4104, doi: 10.1073/pnas.1807261116.

Sime L.C., Risi C., Tindall J.C., Sjolte J., Wolff E.W., Masson-Delmotte V. & Capron E. 2013. Warm climate isotopic simulations: what do we learn about interglacial signals in Greenland ice cores? *Quaternary Science Reviews 67*, 59–80, doi: 10.1016/j.quascirev.2013.01.009.

Stein A.F., Draxler R.R., Rolph G.D., Stunder B.J.B., Cohen M.D. & Ngan F. 2015. NOAA's HYSPLIT atmospheric transport and dispersion modeling system. *Bulletin of the American Meteorological Society 96*, 2059–2077, doi: 10.1175/bams-d-14-00110.1.

Stroeve J.C., Kattsov V., Barrett A., Serreze M., Pavlova T., Holland M. & Meier W.N. 2012. Trends in Arctic sea ice extent from CMIP5, CMIP3 and observations. *Geophysical Research Letters 39*, L16502, doi: 10.1029/2012gl052676.

Stuecker M.F., Bitz C.M., Armour K.C., Proistosescu C., Kang S.M., Xie S.P., Kim D., McGregor S., Zhang W., Zhao S., Cai W., Dong Y. & Jin F.-F. 2018. Polar amplification dominated by local forcing and feedbacks. *Nature Climate Change 8*, 1076–1081, doi: 10.1038/s41558-018-0339-y.

van der Ent R.J. & Tuinenburg O.A. 2017. The residence time of water in the atmosphere revisited. *Hydrology and Earth System Sciences 21*, 779–790, doi: 10.5194/hess-21-779-2017.

Vihma T., Pirazzini R., Fer I., Renfrew I.A., Sedlar J., Tjernström M., Lüpkes C., Nygård T., Notz D., Weiss J., Marsan D., Cheng B., Birnbaum G., Gerland S., Chechin D. & Gascard J.C. 2014. Advances in understanding and parameterization of small-scale physical processes in the marine Arctic climate system: a review. *Atmospheric Chemistry and Physics 14*, 9403–9450, doi: 10.5194/acp-14-9403-2014.

Vihma T., Screen J., Tjernström M., Newton B., Zhang X., Popova V., Deser C., Holland M. & Prowse T. 2016. The atmospheric role in the Arctic water cycle: a review on processes, past and future changes, and their impacts. *Journal of Geophysical Research—Biogeosciences 121*, 586–620, doi: 10.1002/2015JG003132.

Voosen P. 2020. New feedbacks speed up the demise of Arctic sea ice. *Science 369*, 1043–1044, doi: 10.1126/science.369.6507.1043.

Wei Z., Yoshimura K., Okazaki A., Ono K., Kim W., Yokoi M. & Lai C.T. 2016. Understanding the variability of water isotopologues in near-surface atmospheric moisture over a humid subtropical rice paddy in Tsukuba, Japan. *Journal of Hydrology 533*, 91–102, doi: 10.1016/j.jhydrol.2015.11.044.

Xia W., Xie H. & Ke C. 2014. Assessing trend and variation of Arctic sea-ice extent during 1979–2012 from a latitude perspective of ice edge. *Polar Research 33*, 47–53, doi: 10.3402/polar.v33.21249.

Yoshimura K. & Kanamitsu M. 2008. Dynamical global downscaling of global reanalysis. *Monthly Weather Review 136*, 2983–2998, doi: 10.1175/2008mwr2281.1.

Yoshimura K., Kanamitsu M., Noone D. & Oki T. 2008. Historical isotope simulation using reanalysis atmospheric data. *Journal of Geophysical Research—Atmospheres 113*, D19108, doi: 10.1029/2008jd010074.